JMEPEG (2004) 13:619-626
DOI: 10.1361/10599490420647


1059-9495/$19.00

# Effect of Superheat, Mold, and Casting Materials on the Metal/Mold Interfacial Heat Transfer During Solidification in Graphite-Lined Permanent Molds

*K. Narayan Prabhu and K.M. Suresha*

*(Submitted October 21, 2002; in revised form March 21, 2004)*

**Heat transfer during the solidification of an Al-Cu-Si alloy (LM4) and commercial pure tin in single steel, graphite, and graphite-lined metallic (composite) molds was investigated. Experiments were carried out at three different superheats. In the case of composite molds, the effect of the thickness of the graphite lining and the outer wall on heat transfer was studied. Temperatures at known locations inside the mold and casting were used to solve the Fourier heat conduction equation inversely to yield the casting/mold interfacial heat flux transients. Increased melt superheats and higher thermal conductivity of the mold material led to an increase in the peak heat flux at the metal/mold interface. Factorial experiments indicated that the mold material had a significant effect on the peak heat flux at the 5% level of significance. The ratio of graphite lining to outer steel wall and superheat had a significant effect on the peak heat flux in significance range varying between 5 and 25%. A heat flux model was proposed to estimate the maximum heat flux transients at different superheat levels of 25 to 75 °C for any metal/mold combinations having a thermal diffusivity ratio ($\alpha_R$) varying between 0.25 and 6.96. The heat flow models could be used to estimate interfacial heat flux transients from the thermophysical properties of the mold and cast materials and the melt superheat. Metallographic analysis indicated finer microstructures for castings poured at increased melt superheats and cast in high-thermal diffusivity molds.**

**Keywords:** composite mold, graphite lining, interfacial heat flux, superheat, thermal diffusivity

## 1. Introduction

The use of chills during the freezing of long-freezing-range aluminum alloys enhances the rate of heat transfer from the casting to the chill material and promotes directional solidification.[1] Graphite has good thermal conductivity, and the use of graphite as a mold/chill material results in the rapid solidification of the alloy being cast and imparts a dense smooth surface to the cast product. It is also possible to cast alloys with higher melting points such as titanium and copper in permanent graphite molds.[2] In addition, graphite acts as a lubricant, and, hence, graphite molds normally do not require frequent mold coating as is the case with ferrous dies. Graphite mold/chill material prevents premature solidification and does not wrap or distort during casting, since it has a low coefficient of thermal expansion compared with ferrous dies.[3] In summary, the use of a graphite lining for a metallic mold has the following significant advantages.[4]

- Graphite provides a nonwetting surface for the casting and serves as a reservoir for the casting lubricant. Since it experiences little wear, it reduces mold maintenance, leading to longer mold life.
- Water cooling of the outer die provides good heat transfer rates.
- Graphite is, however, a brittle material, and in composite molds the presence of an outer metallic layer enables the graphite lining to resist mechanical shock during handling.
- Graphite facilitates the easy replacement of the lining and, hence, leads to lower maintenance costs.

Furthermore, graphite has a low coefficient of thermal expansion ($4.65 \times 10^{-6}$/°C), and this results in high thermal shock resistance. Graphite-lined composite molds are currently being explored for the direct-chill and continuous casting of nonferrous alloys, for the casting of titanium and titanium-based alloys, for the gravity and die casting of aluminum- and zinc-based alloys, for the up-casting of brass and copper, and for the casting of rail wheels.[5,6]

Sully[7] studied the effect of casting size, casting alloy, mold material, and mold geometry on the heat transfer coefficient and concluded that the mold geometry affects the heat transfer coefficient significantly, while the mold material and casting alloy have only a small effect on it. Further, the size of the casting controls the temporal variation of the heat transfer coefficient. While the casting surface temperature has a large effect on heat transfer coefficient, the mold temperature has little effect on it. Nishida et al.[8] determined the heat transfer coefficient for pure aluminum and an Al-13.2Si alloy that were cast into graphite-coated molds with about 0.01 mm of graphite. It was found that the level of mold constraint had a large effect on the heat transfer coefficient, while alloy composition had only a minor effect.

Strezov and Herbertson[9] studied the heat transfer characteristics between a copper substrate embedded in a flat wedge

**K. Narayan Prabhu** and **K.M. Suresha,** Department of Metallurgical & Materials Engineering, National Institute of Technology Karnataka, Surathkal, P.O. Srinivasnagar 575 025, India. Contact e-mail: prabhukn_2002@yahoo.co.in.

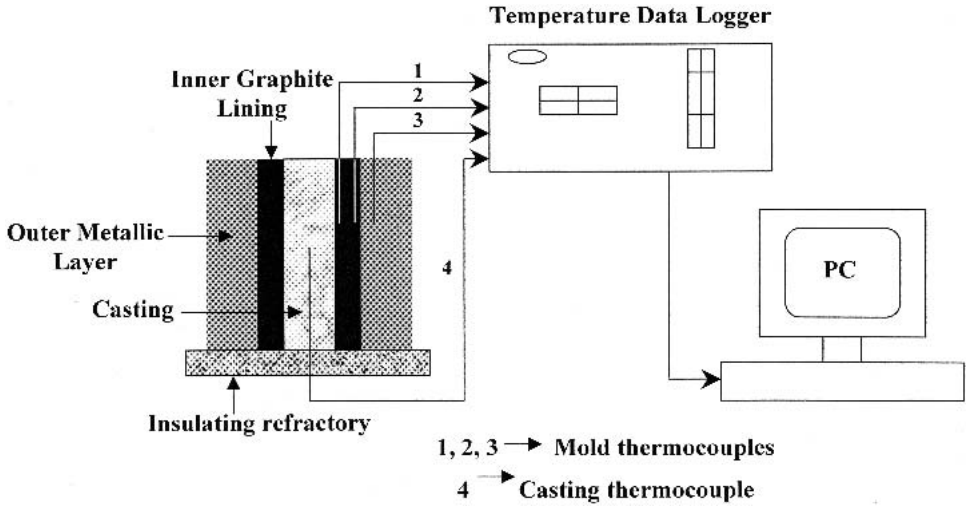


**Fig. 1** Schematic of the experimental setup for solidification in a graphite-lined steel (composite) mold. PC, personal computer

**Table 1 Mold dimensions**

| Type of mold and designation | Inner wall material/ thickness, mm | Outer wall material/ thickness, mm |
|---|---|---|
| Steel mold | … | … |
| Graphite mold | … | … |
| Composite mold, CM-1 | Graphite/15 | Steel/20 |
| Composite mold, CM-2 | Graphite/25 | Steel/10 |
| Composite mold, CM-3 | Graphite/10 | Steel/25 |
| Graphite-lined copper mold, CM-4 | Graphite/15 | Copper/20 |

Note: Outer diameter of the mold, 100 mm; hole diameter, 30 mm; height of mold, 120 mm

and a stainless steel bath into which the wedge was rapidly immersed. Substrate texture, gas atmosphere, immersion velocity, and melt superheat were investigated for their effect on heat transfer. Melt superheat was seen to have a significant effect on the peak heat flux in the initial 50 ms of melt/substrate contact. Increased superheats resulted in decreased peak heat fluxes. It was concluded that the peak heat flux was a quantitative reflection of the initial melt/substrate contact, which correlated strongly with nucleation behavior in the solidified sample. The maximum heat flux was higher for textured surfaces than for smooth ones.

Netto et al.[10] studied the heat transfer between a solidifying light metal strip and a moving substrate. It was found that higher superheat led to an increase in the peak heat flux. They observed that the interfacial heat flux depended on the thickness of the strips, the initial superheat, and the properties of coating.

Prabhu and Griffiths[11] compared the heat flux transients during the solidification of cast iron in a graphite mold to that in a sand mold. Use of the graphite molds resulted in a well-defined peak heat flux, which was attributed to the higher rigidity and thermal conductivity of the graphite material, causing the early formation of a stable solid shell. Further, the contribution of conduction to heat transfer was significant in the graphite molds, contributing as much as 90% to the overall heat transfer. For sand molds, the conduction and radiation modes of heat transfer were dominant.

The benefits of graphite and metallic materials are advantageously combined in a composite mold, providing better casting yields and higher productivity. In addition, the resistance offered by the graphite-lining/outer-metallic-wall interface to heat transfer during solidification was found to be negligible.[12] A heat transfer model was proposed to estimate the heat flux transients during solidification in the composite mold; however, this model does not take into account the effect of the superheat of the melt and the thermal properties of the mold on the resulting microstructure.

In the present investigation, heat transfer at the casting/mold interface was assessed during the solidification of the Al-3Cu-4.5Si alloy (LM4, hereafter referred to as Al-Cu-Si) and commercial pure tin in single steel, graphite, and graphite-lined metallic molds at three different superheats. The aim of study was to assess the effect of mold material, superheat, and the ratio of the thickness of the inner graphite lining to the outer wall on the thermal behavior of the casting and the mold. Heat flux transients were estimated using an inverse-modeling approach for all casting/mold and superheat combinations. An attempt has been made to correlate the effect of the thermal diffusivity of the mold and casting materials and superheat temperature on the heat flux and fineness of the metallurgical microstructure of the cast material.

## 2. Experimental Procedures

The composite mold consisted of a graphite inner cylinder and a mild-steel/copper outer cylinder. The graphite block was initially cut to approximate size and then turned to exact dimensions. A hole, 30 mm in diameter, was drilled in the cylindrical graphite block. The mild steel/copper was also turned to the required dimensions followed by the boring operation. The dimensions of the molds were selected such that an interference fit was obtained between the inner graphite and outer mild steel/copper cylinders. The wall thickness of the composite mold was equal to the sum of the wall thickness of the graphite lining and the outer metal cylinders. The single ma-

**Table 2 Thermophysical properties of the casting and mold materials**

| Material | Density (ρ), kg/m$^3$ | Thermal conductivity ($k$), W/mK | Specific heat ($C_p$), J/kgK | Thermal diffusivity ($\alpha = k/(\rho C_p)$), m$^2$/s |
|---|---|---|---|---|
| **Casting material** | | | | |
| Al-Cu-Si (LM 4) | 2690 | 194 | 1162 | $6.206 \times 10^{-5}$ |
| Tin | 7300 | 65 | 226 | $3.94 \times 10^{-5}$ |
| **Mold material** | | | | |
| Steel | 7700 | 42 | 611 | $0.892 \times 10^{-5}$ |
| Graphite | 1890 | 174.5 | 670 | $13.8 \times 10^{-5}$ |
| Copper | 8960 | 386 | 383.1 | $11.234 \times 10^{-5}$ |

terial molds of graphite and mild steel were similarly prepared. Table 1 gives the dimensions of the molds used in the present investigation. The casting diameter and height were 30 and 120 mm, respectively. Figure 1 shows a schematic of the experimental setup.

On the top surface of the molds, holes of 1.5 mm diameter were drilled to a depth 45 mm at various locations from the casting/mold interface for the insertion of thermocouples to monitor the mold thermal history. Two varieties of K-type thermocouples were used for the experiment. Stainless steel sheathed thermocouples of 1 mm diameter were used in the mold, and 0.45 mm thermocouple wires, which were inserted in twin bored ceramic beads of 5 mm diameter, were adopted for monitoring the cooling behavior of the solidifying casting. The sheathed thermocouples were reusable, and the ceramic beaded thermocouple located in the casting was sacrificial.

The metal melt stock was melted in a fireclay crucible using a resistance furnace. The beaded thermocouple was located such that the tip of the thermocouple was positioned exactly at the geometric center of the mold. It was inserted through a hole provided at the center of a low-conductivity refractory brick that was placed at the bottom of the mold. The top surface of the mold was insulated with ceramic wool to prevent the dissipation of heat in the vertical direction. The melt was superheated to the required temperature with pouring carried out at three different superheat temperatures (i.e., 25, 50, and 75 °C above the melting point of the aluminum or tin alloy). A portable temperature data logger was used for acquiring the temperature data from the instrumented molds and the casting. Temperature data were collected until the end of solidification.

Table 2 gives the thermophysical properties of the casting and mold materials used in the experiments. The thermophysical properties of the composite molds used in the experiments can be calculated from knowledge of the thermophysical properties of the separate mold materials. The following equation was used to determine the thermal conductivity of the graphite-lined steel/copper composite mold.

$$\frac{1}{k_{\text{composite}}} = \frac{D_g}{k_g} + \frac{D_m}{k_m} \quad \text{(Eq 1)}$$

where

$$D_g = \frac{t_g}{t_t} \quad \text{and} \quad D_m = \frac{t_m}{t_t}$$

In these equations, $t_g$ is the graphite lining thickness, $t_m$ is the outer steel/copper wall thickness, and $t_t$ is the total wall thickness of the composite mold. The density and specific heat of the composite molds were calculated in a similar manner.

Specimens for metallographic examination were prepared using sections taken at 60 mm from the bottom of each casting. Surface preparation was initially carried out on a belt grinder with subsequent polishing taking place on different grades of emery paper. Final surface preparation was carried out on a polishing disc to obtain a scratch-free finish using lavigated alumina as the polishing abrasive. The polished Al-Cu-Si and tin specimens then were etched with appropriate etchants.

## 3. Results and Discussion

Figure 2 shows the typical casting/mold thermal history during the solidification of Al-Cu-Si in a graphite-lined metallic mold. The temperature recorded by the casting thermocouple TC1 showed the maximum temperature after a time interval of 3-4 s. The gap of 3-4 s that it takes the thermocouple to record the peak temperature was probably due to the time needed to fill the mold and the subsequent response time for the thermocouple to reach equilibrium. The liquid metal cooled rapidly from the pouring temperature to the freezing temperature, and this was accompanied by a sharp change in the slope near the freezing temperature due to the evolution of the latent heat of fusion. The mold thermal history recorded by thermocouples TC2, TC3, and TC4 indicated that the location near the mold interface (TC2) heated rapidly after the liquid metal was poured into the mold. The temperature reached a peak and then decreased at a slower rate compared with the initial rate of heating.

The cooling rate of the casting was calculated from the time required to cool from the liquidus temperature to the solidus temperature. It was found that the cooling rate of the casting varied from mold to mold. For example, the cooling rates of Al-Cu-Si poured using a 25 °C superheat in steel, CM-3, CM-1, CM-2, graphite, and CM-4 molds were 14, 17, 20, 22, 26, and 41 °C/s, respectively. This showed that the mold material had a significant effect on the cooling behavior of the solidifying casting. Higher cooling rates for the castings were obtained with an increase in the thermal conductivity of the mold material.

It was observed that the heating rate as calculated from the temperature data recorded by thermocouple TC2 located near the interface varied from mold to mold. For example, the heat-

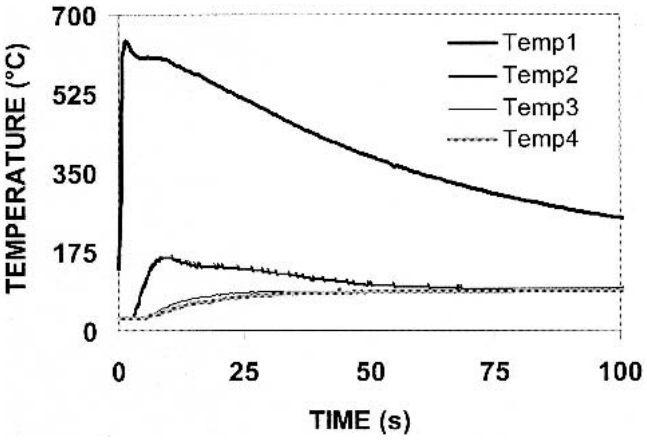


**Fig. 2** Temperature-time curves during the solidification of the Al-Cu-Si (LM4) alloy in a steel mold

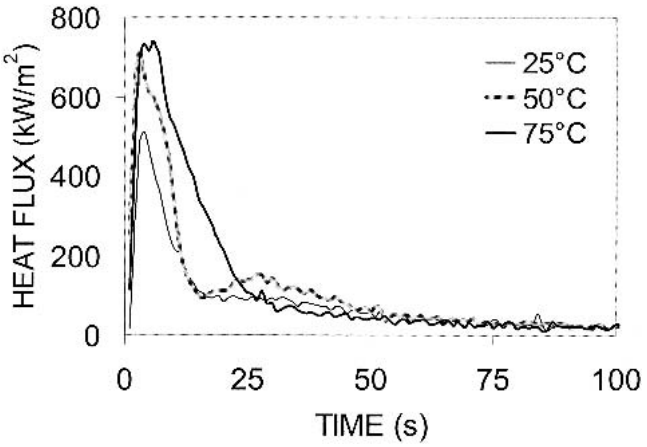


**Fig. 3** Heat flux transients for Al-Cu-Si alloy (LM4) solidifying in a steel mold

ing rates at the time of the occurrence of peak temperatures for the steel, CM-3, CM-1, CM-2, graphite, and CM-4 molds, for Al-Cu-Si poured at a 25 °C superheat, were 7, 10, 17, 20, 25, and 27 °C/s, respectively. The difference is attributed to the varying thermal diffusivity for the different mold materials. Thermal diffusivity was a maximum for the graphite-lined copper composite (CM-4) mold ($15.7 \times 10^{-5}$ m$^2$/s) and a minimum for the steel mold ($0.892 \times 10^{-5}$ m$^2$/s).

Similarly, the superheat had a significant effect on the peak temperature recorded by thermocouple TC2, which was located near the interface. For example, the peak temperatures recorded by the thermocouple TC2 for Al-Cu-Si poured at 25, 50, and 75 °C superheats in steel and CM-2 molds were 93, 128, and 160 °C, and 151, 160, and 162 °C, respectively. The increase in pouring temperature increased the fluidity of the liquid metal and probably improved the wettability of the melt on the mold surface. The temperature remained constant after a period of about 40 s. At locations away from the interface, the temperature gradually increased and remained constant after about 300 s for the Al-Cu-Si and after about 150 s for the tin.

Casting material also had a significant effect on the thermal behavior of the molds during solidification. For example, the heating rates at location TC2 (near the interface) during solidification of Al-Cu-Si and tin in the steel mold, when poured at 25, 50, and 75 °C superheats, were 7, 9, and 10 °C, and 4, 5, and 6 °C, respectively. This was because the latent heat of fusion for tin (59.5 kJ/kg) is substantially lower than that for the Al-Cu-Si (389 kJ/kg).

The nonlinear estimation of Beck,[13] which utilizes a numerical approach to estimate the surface heat flux density from knowledge of the measured temperatures inside the heat conduction solid, was adopted in this work. This approach analyzes the transient heat transfer at the surface. The thermocouples located near the casting/mold interface were used as the monitored temperature node, and the location of the thermocouple near the mold surface in contact with the solidifying casting was used as the boundary node.

Figures 3-6 show the effect of superheat on the heat flux at the interface for a typical metal/mold interface. The heat flux increased rapidly as the liquid metal filled the mold cavity and reached a peak value after a time of about 2 s. The peak flux

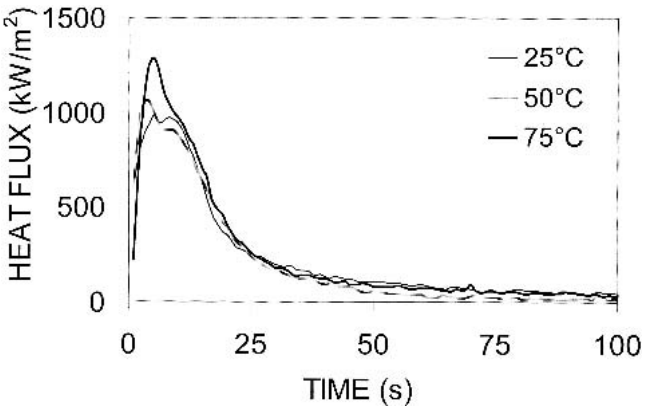


**Fig. 4** Heat flux transients for Al-Cu-Si alloy (LM4) solidifying in a graphite-lined steel mold (CM-1)

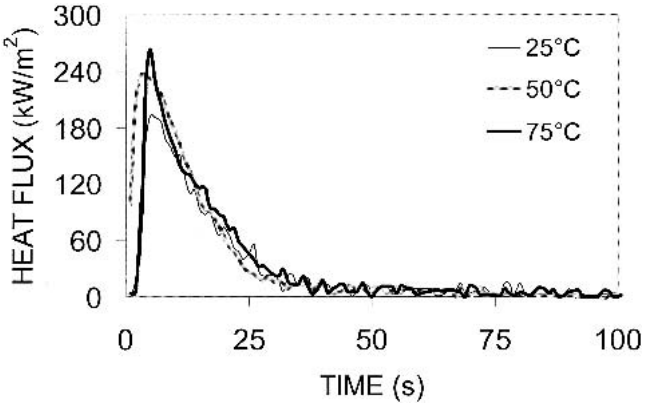


**Fig. 5** Heat flux transients for tin solidifying in a steel mold

could be associated with the formation of a solidified shell near the casting/mold interface. The formation of a solidified shell is accompanied by the evolution of additional heat through fusion. Further, the thermal conductivity of the solidified shell is greater than the thermal conductivity of the liquid metal in

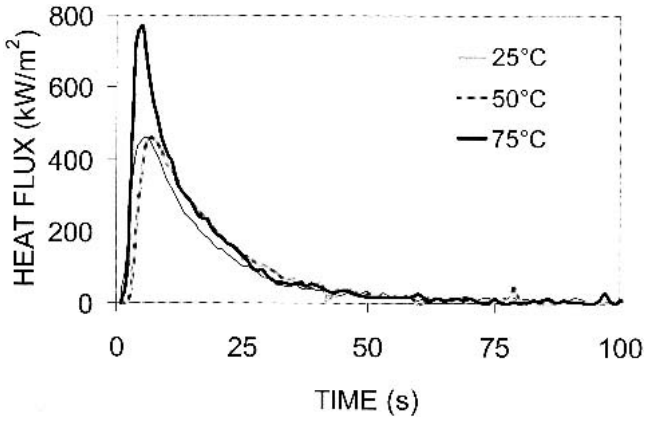


**Fig. 6** Heat flux transients for tin solidifying in a graphite-lined steel mold (CM-1)

contact with the inner surface of the mold wall. In the case of Al-Cu-Si, the thermal conductivity of the alloy in the liquid and solid states is 90 and 194 W/mK, respectively. The initially formed casting skin is weak, and it may be pushed against the mold wall by the metallostatic pressure of the liquid metal. This may result in an intimate contact between the mold wall and the casting skin. Since a good contact is made between the casting skin and the mold, heat flux rapidly rises to a maximum. At the same time, the casting skin temperature drastically drops. As the thickness of the solidified shell increases with time, it gains sufficient strength to resist metallostatic pressure. The deformation of the initial solidified layer has been observed by Dong et al.[14] The contraction of the casting skin away from the mold leads to nonconforming contact at the interface. The heat flux drastically decreases due to the change in the casting/mold interfacial condition, i.e., from a conforming contact to a nonconforming contact.

### 3.1 Factorial Experiments

It was found that for Al-Cu-Si solidifying in all types of molds, peak heat flux transients increased with the increase in melt superheat. The increased heat flux transients with an increase in melt superheat might be attributed to:

- Improved interfacial contact between the melt and the mold surface, and
- Increased initial driving force ($T_s - T_m$) for heat transfer across the interface.

However, in the case of tin solidifying in composite molds, a mixed trend was observed. For example, the peak fluxes were 828, 736, and 1017 kW/m$^2$ at 25, 50, and 75 °C superheat levels, respectively, for the tin solidifying in the CM-4 mold.

To assess the statistical significance of the superheat, mold material, and ratio of the thickness of the graphite lining to the outer steel wall on estimated peak heat rates, $2^3$ factorial experiments were carried out. A detailed procedure for carrying out factorial experiments is given in the study by Montgomery.[15]

Tables 3 and 4 give the peak heat flux data and analysis of variance for Al-Cu-Si solidifying in steel, graphite, and graphite-lined copper molds. Tables 5 and 6 give the peak heat flux data and the analysis of variance for tin solidifying in steel molds lined with graphite of varying thicknesses. From the results of the factorial experiments, it was found that the mold material had a significant effect on peak heat flux at the 5% level of significance. The ratio of the thickness of the inner graphite lining to that of the outer steel wall and the superheat had a significant effect on peak heat flux in the range of significance between 5% and 25%.

**Table 3 Peak heat flux data for Al-Cu-Si (LM4) solidified in steel, graphite, and graphite-lined copper molds**

| Mold type | $q_{max}$, kW/m$^2$ 25 °C superheat | 50 °C superheat | 75 °C superheat | Total Yi. |
|---|---|---|---|---|
| Steel | 512.7 | 715.8 | 740.3 | 1,968.8 |
| Graphite | 928.3 | 1188.5 | 1693.0 | 3,809.8 |
| Graphite-lined copper | 1179.2 | 2148.2 | 2553.5 | 5,880.9 |
| Yj. | 2620.2 | 4052.5 | 4986.8 | 11,659.5 |

$q_{max}$, peak heat transfer rate; Yi, total of all observations under the ith level of mould type factor; Yj, total of all observations under jth level of superheat factor

**Table 4 Analysis of variance (ANOVA) table for the heat flux data given in Table 3**

| Source of variance | Sum of squares | Degrees of freedom | Mean square | $F_0$ |
|---|---|---|---|---|
| Mold type | 2,553,719 | 2 | 1,276,859 | 89.52 |
| Superheat | 947,175 | 2 | 473,587 | 33.20 |
| Nonadditivity | 340,803 | 1 | 340,803 | 232.83 |
| Error | 42,791 | 3 | 14,263 | … |
| Total | 3,884,489 | 8 | … | … |

Note: At 5% significance level, $F_{0.05,\ 1,\ 3} = 10.13$ (from standard F-tables). Since $F_0 > F_{0.05,\ 1,\ 3}$, both superheat and mold material have a significant effect on peak heat flux

### 3.2 Modeling of Heat Flux Transients

To model the peak heat transfer rate at the casting/mold wall interface at different levels of superheat, a dimensionless ratio of thermal diffusivities was defined as

$$\alpha_R = \frac{\alpha_{casting}}{\alpha_{mold}} \quad \text{(Eq 2)}$$

The effect of the thermal diffusivity ratio ($\alpha_R$) on peak heat flux transients at different superheat levels is shown in Fig. 7 and can be described by a regression equation of the form:

$$\frac{q_{max} tA}{ML_f + MCp\Delta T} = 0.3332(\alpha_R)^{-0.3907} \quad \text{(Eq 3)}$$

where $L_f$ is the latent heat liberated, $q_{max}$ is the peak heat

**Table 5 Peak heat flux data for tin solidifying in composite molds**

| Thickness ratio | $q_{max}$, kW/m$^2$ 25 °C superheat(a) | 50 °C superheat(a) | 75 °C superheat(a) | Total Yi. |
|---|---|---|---|---|
| 0.4, CM-3 | 174.9 | 172.5 | 231.1 | 578.5 |
| 0.75, CM-1 | 459.5 | 457.9 | 772.2 | 1689.6 |
| 2.5, CM-2 | 280.7 | 306.0 | 328.6 | 915.3 |
| Yj. | 915.1 | 936.4 | 1331.9 | 3183.4 |

(a) Temperature above the melting point
Yi, total of all observations under the ith level of thickness ratio factor; Yj, total of all observations under the jth level of superheat factor

**Table 6 Analysis of variance (ANOVA) table for the heat flux data given in Table 5**

| Source of variance | Sum of squares | Degrees of freedom | Mean square | $F_0$ |
|---|---|---|---|---|
| Thickness ratio | 216,369 | 2 | 108,185 | 71.23 |
| Superheat | 36,730 | 2 | 18,365 | 12.09 |
| Nonadditivity | 27,566 | 1 | 27,566 | 18.15 |
| Error | 4,556 | 3 | 1,519 | … |
| Total | 285,221 | 8 | … | … |

Note: At 5% significance level, $F_{0.05,\ 1,\ 3} = 10.13$ (from standard F-Table). Since $F_0 > F_{0.05,\ 1,\ 3}$ both superheat and thickness ratio have a significant effect on the peak heat flux.

transfer rate during the solidification of the casting, $t$ is the time of occurrence of the peak heat flux, $A$ is the interfacial contact area between the casting and the mold, $M$ is the mass of the casting, $C_p$ is the specific heat, and $\Delta T$ is equal to $(T_s - T_m)$. Equation 2 is dimensionally consistent.

The correlation coefficient for the above equation is 0.74, and the equation is valid for thermal diffusivity values ranging from 0.25-6.96. The left-hand side of Eq 3 is called the dimensionless interfacial heat flux transient, and it denotes the total heat that can be extracted from the casting prior to complete solidification. The above equation could be used to estimate the peak heat flux transients for any metal/mold combination from knowledge of their thermophysical properties. Equation 3 suggests that with an increase in the $\alpha_R$, the ability of the mold to extract heat from the casting decreases.

The heat flux was normalized with respect to the peak heat flux, and its variation with time for different metal/mold and superheat combinations is shown in Fig. 8. The variation can be approximated by a best-fit polynomial equation of the following form:

$$\frac{q}{q_{max}} = -2 \times 10^{-5} t^3 + 0.0019 t^2 - 0.0074 t + 1.092 \qquad \text{(Eq 4)}$$

The correlation coefficient for the best-fit equation was 0.92.

To estimate the heat flux transients after the occurrence of peak flux from the proposed empirical equations, the following methodology was adopted.

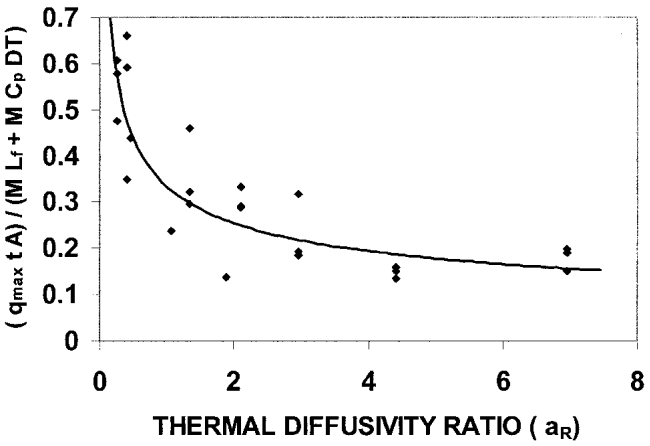


**Fig. 7** Effect of $\alpha_R$ on dimensionless peak heat flux transients

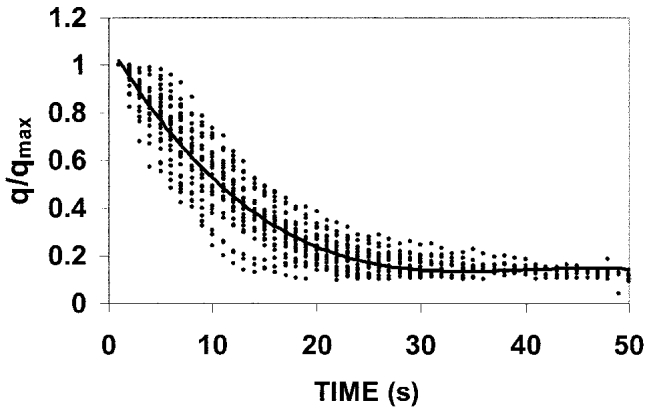


**Fig. 8** Variation of normalized heat flux with time

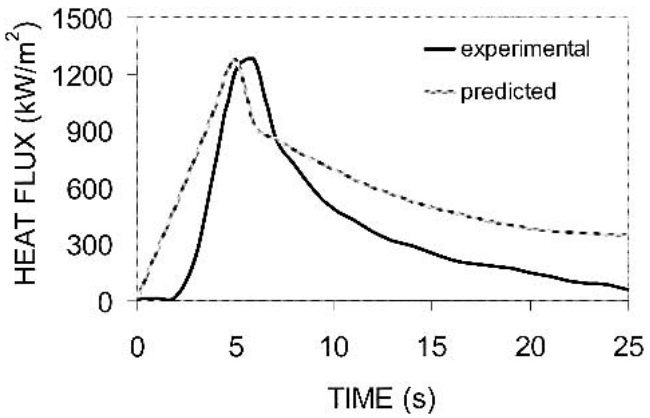


**Fig. 9** Comparison of predicted and experimental heat flux transients during the solidification of zinc solidifying in a graphite-lined steel mold (CM-1)

1) The peak heat flux ($q_{max}$) was calculated from the $\alpha_R$ using Eq 3.
2) The time of occurrence of the peak heat flux was taken as 5 s, and the heat flux values for the initial 5 s were estimated by linear interpolation.

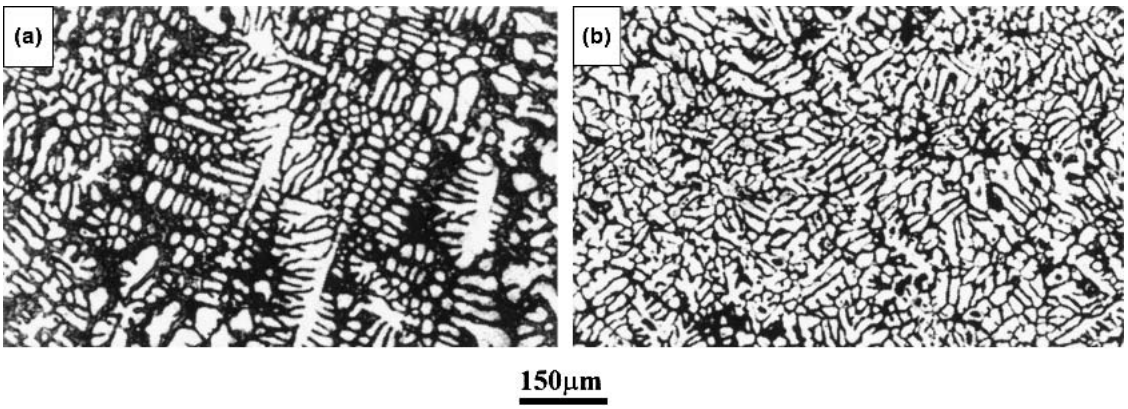


**Fig. 10** Microstructures of the Al-Cu-Si alloy cast in a composite mold (CM-2): **(a)** superheat, 25 °C; **(b)** superheat, 75 °C

3) The heat flux transients after the occurrence of the peak flux can be approximated using Fig. 8 and Eq 4.

Although the heat transfer model presented above gives only an approximate estimate of the heat flux transients, it can be used to assess the heat transfer during the solidification of nonferrous alloys solidifying in various metal/mold combinations at different superheat levels, for which the $\alpha_R$ lies between 0.25 and 6.96.

Figure 9 shows the comparison of predicted and experimental heat flux transients during the solidification of zinc solidifying in a graphite-lined steel mold (CM-1) at a superheat temperature of 50 °C. Predicted heat flux transients were in good agreement with the heat flux values estimated by inverse analysis.

### *3.3 Cast Microstructures*

Figure 10(a) and (b) show the micrographs of Al-Cu-Si cast in a composite mold (CM-2) at superheat levels of 25 and 75 °C, respectively. It was found that with an increase in the thermal diffusivity of mold material and melt superheat, the mean secondary dendrite arm spacing (SDAS) decreased. The increase in the thermal diffusivity of the mold material resulted in higher heat extraction from casting, which led to increased dendrite fineness. The increase in fluidity and lower surface tension at higher superheats might have resulted in improved wetting of the mold surface by the liquid metal, leading to a finer microstructure. This is in agreement with the results of Netto et al.[10] and Muojekwu et al.[16] However, Strezov and Herbertson[9] observed coarser dendrites with increasing melt superheat, which they attributed to the reduced driving force for nucleation at the higher superheat temperatures.

Figure 11(a) and (b) show the micrographs of the tin cast in CM-2 molds at superheat levels of 25 and 75 °C, respectively. Finer-grained structures were obtained with the increase in melt superheat and the increase in thermal diffusivity of the mold material. Similar results were obtained for other molds as well.

## 4. Conclusions

The casting/mold interfacial heat transfer during the solidification of Al-Cu-Si and commercial pure tin in single steel, graphite, and graphite-lined metallic molds was assessed using an inverse analysis technique. Based on the results and discussion, the following conclusions were drawn:

- Heat flux transients showed a peak immediately after pouring, and the peak heat flux could be associated with the formation of an initial solidified shell in conforming contact with the inner surface of the mold. The time of occurrence of the peak heat flux was nearly 5 s after pouring. The decrease in the heat flux after the occurrence of the peak was attributed to the transformation of the interfacial condition from conforming to nonconforming contact.
- The increase in the melt superheat resulted in a higher peak flux due to improved casting/mold interfacial contact and the increased fluidity and wettability of the liquid metal.
- Factorial experiments indicated that mold material had a significant effect on peak heat flux at the 5% level of significance. However, the effect of the superheat and the ratio of the thickness of the inner graphite lining to the outer steel wall was significant only in the range of significance levels varying between 5% and 25%.
- The variation of peak heat flux transient was modeled as a function of the ratio of the thermal diffusivity of the casting to the mold and is represented by the power equation

$$\frac{q_{max}tA}{ML_f + MCp\Delta T} = 0.3332(\alpha_R)^{-0.3907}$$

  The peak heat transfer regression model can be used to calculate the maximum heat transfer at the casting/mold interface for any combination of metal-mold type having an $\alpha_R$ between 0.26 and 6.96 when metal is poured at superheat levels ranging from 25-75 °C.
- The heat flux transients, after the occurrence of the peak heat flux, were normalized with respect to the peak heat flux and were modeled as a function of time. This is best represented by a polynomial equation. The heat flow models were validated, and the predicted values were found to be in good agreement with experimentally measured data.
- An increase in melt superheat resulted in finer microstructures due to improved contact at the casting/mold wall interface. An increase in the thermal diffusivity of the

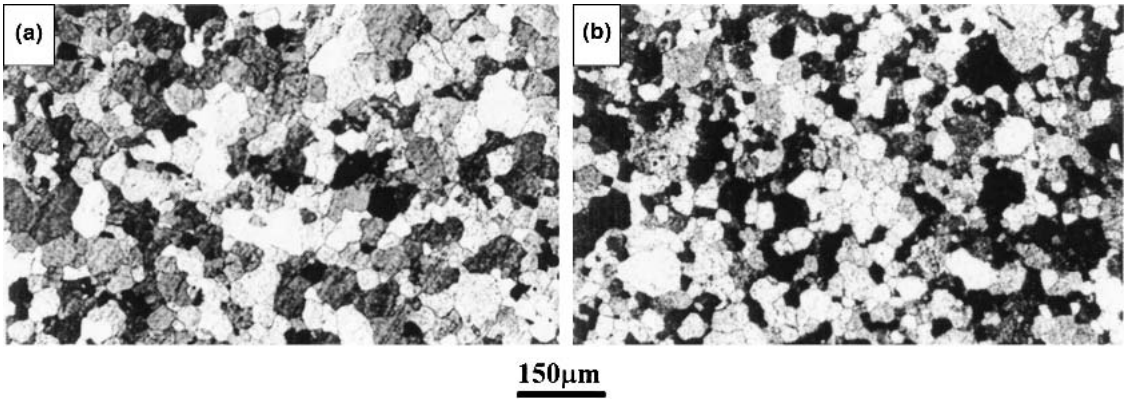


**Fig. 11** Microstructures of tin cast in a composite mold (CM-2): **(a)** superheat, 25 °C; **(b)** superheat, 75 °C

mold material also resulted in finer microstructures. Microstructural fineness was at a maximum during solidification in the graphite-lined copper mold (CM-4) at a superheat level of 75 °C and was at a minimum during solidification in steel molds at a superheat level of 25 °C.

## References


1. C.V. Kutumba Rao and V. Panchanathan, End Chills Influence on Solidification Soundness of Al-Cu-Si (LM 4) Alloy Castings, *AFS Trans.,* Vol 81, 1970, p 110-114
2. R.W. Heine, C.R Loper, and P.C Rosenthal, *Principles of Metal Casting,* Tata McGraw-Hill, New Delhi, 1976
3. W. Mihaichuk, An Introduction to Graphite Permanent Mold Castings, *Mod. Cast.,* March 1986, p 33-37
4. "Innovative Casting Systems for the Aluminium Industry," technical literature, WagStaff, Inc., WA, 2000
5. "Griffins Process, Pressure Pouring in a Graphite Mold," http://www.griffinwheel.com, Griffin Wheel Co., Chicago; (accessed June 2002)
6. K. Harkki and J. Miettinen, Mathematical Modelling of Copper and Brass Up-Casting, *Metall. Mater. Trans.,* Vol 30B, 1999, p 75-89
7. L.J.D. Sully, The Thermal Interface Between Casting and Chill Molds, *AFS Trans.,* Vol 84, 1976, p 735-744
8. Y. Nishida, W. Droste, and S. Engler, The Air-Gap Formation Process at the Casting-Mold Interface and the Heat Transfer Mechanism Through the Air Gap, *Metall. Trans. B,* Vol 16B, 1986, p 833-844
9. L. Strezov and J. Herbertson, Experimental Studies of Interfacial Heat Transfer and Initial Solidification Pertinent to Strip Casting, *ISIJ Int.,* Vol 38, 1998, p 959-966
10. P.G.Q. Netto, R.P. Taveres, M. Isac, and R.I.L. Guthrie, A Technique for the Evaluation of Instantaneous Heat Fluxes for the Horizontal Strip Casting of Aluminium Alloys, *ISIJ Int.,* Vol 41, 2001, p 1340-1349
11. K.N. Prabhu and W.D. Griffiths, Assessment of Metal/Mould Interfacial Heat Transfer During Solidification in Cast Iron, *Mater. Sci. Forum,* Vol 1329-1330, p 455-460
12. K.N. Prabhu, H. Mounesh, K.M. Suresha, and A.A. Ashish, Casting/Mould Interfacial Heat Transfer During Solidification in Graphite, Steel and Graphite Lined Steel Moulds, *Int. J. Cast Metals Res.,* Vol 15, 2003, p 565-572
13. J.V. Beck, Non Linear Estimation Applied to the Non Linear Heat Conduction Problem, *J. Heat Transfer,* Vol 13, 1970, p 703-716
14. S.-X. Dong, E. Niyama, K. Anzai, and N. Matsumoto, Free Deformation of the Initial Solid Layer of Some Non-Ferrous Alloys, *Cast Metals,* Vol 6, 1993, p 115-120
15. D.C. Montgomery, The $2^k$ Factorial Design, *Design and Analysis of Experiments,* John Wiley, 1991, p 270-309
16. C.A. Muojekwu, I.V. Samarasekara, and J.K. Brimacombe, Heat Transfer and Microstructure During Early Stages of Metal Solidification, *Metall. Trans. B,* Vol 26B, 1995, p 361-381